



Skin surface lipids photo-oxidation: A vibrational spectroscopy study

Ali Assi, Rime Michael-jubeli, Carine Jacques-jamin, H       Duplan, Arlette Baillet-guffroy, Ali Tfayli

► To cite this version:

Ali Assi, Rime Michael-jubeli, Carine Jacques-jamin, H       Duplan, Arlette Baillet-guffroy, et al.. Skin surface lipids photo-oxidation: A vibrational spectroscopy study. Journal of Raman Spectroscopy, 2023, 10.1002/jrs.6504 . hal-04059468

HAL Id: hal-04059468

<https://hal.science/hal-04059468>

Submitted on 5 Apr 2023

HAL is a multi-disciplinary open access archive for the deposit and dissemination of scientific research documents, whether they are published or not. The documents may come from teaching and research institutions in France or abroad, or from public or private research centers.

L'archive ouverte pluridisciplinaire **HAL**, est destin     au d    t et    la diffusion de documents scientifiques de niveau recherche, publi     ou non,   manant des   tablissements d'enseignement et de recherche fran  ais ou   trangers, des laboratoires publics ou priv    .

RESEARCH ARTICLE

Skin surface lipids photo-oxidation: A vibrational spectroscopy study

Ali Assi¹  | Rime Michael-Jubeli¹ | Carine Jacques-Jamin² |
Hélène Duplan² | Arlette Baillet-Guffroy¹ | Ali Tfayli¹

¹Lipides: Systèmes Analytiques et Biologiques, Université Paris-Saclay, Orsay, France

²Center of Research Pierre Fabre Dermo-Cosmetics (PFDC), Toulouse, France

Correspondence

Ali Tfayli, Chimie Analytique Pharmaceutique (FKA EA4041 Groupe de Chimie Analytique de Paris-Sud), Université Paris-Sud, Université Paris-Saclay, 91400 Orsay, France.
Email: ali.tfayli@universite-paris-saclay.fr

Abstract

Skin surface lipid (SSL) film is a mixture of sebum and epidermal lipids protecting the skin from the effects of the environment such as solar radiation. SSLs are a suitable target and scavenger for all reactive oxygen species (ROS) generated in the skin. In the SSLs, vitamin E has been identified as one of the main antioxidants that can capture ROS. This paper is the third part of a global study that evaluates the effect of solar radiation on the lipid classes that constitute SSLs. In the first two parts, the effect of solar radiation on fatty acids and triglycerides was studied using vibrational spectroscopy. In this part, the effect on the other lipid classes such as squalene (SQ), cholesterol (Chol), and wax ester (WE) (Palmitoleyl Palmitate) was studied and then the behavior of vitamin E under solar radiation was monitored. Finally, SSLs were irradiated and analyzed using vibrational spectroscopy and HT-GC/MS to respectively follow the oxidation process and to identify the first target of solar radiation in SSLs. When irradiated alone, SQ oxidation process was detectable only after 2430 J/cm² dose. Similar observations were obtained for vitamin E (after 1620 J/cm²). No changes were observed on the cholesterol and on the wax ester (Palmitoleyl Palmitate). In contrast, when extracted human SSLs film was irradiated, the more marked modifications were observed on SQ. This confirmed the antioxidant role of SQ by scavenging free radicals generated from the oxidation of polyunsaturated fatty acids (PUFA).

KEYWORDS

lipid peroxidation, skin surface lipids, solar radiation, vibrational spectroscopy

1 | INTRODUCTION

The *stratum corneum*, the upper layer of the epidermis, consists of corneocytes embedded in a lipid matrix.^[1–3] It is responsible for the formation and maintenance of skin barrier against water loss and environmental

stresses such as ultraviolet (UV) solar radiation.^[4–6] The protective role of SC against UV is mainly due to the reflection or the absorption of the radiation.^[7]

The surface of the SC the hydrolipidic film, composed of sweat and skin surface lipids (SSLs), represents the utmost barrier with the external environment.^[8]

This is an open access article under the terms of the [Creative Commons Attribution-NonCommercial-NoDerivs](https://creativecommons.org/licenses/by-nc-nd/4.0/) License, which permits use and distribution in any medium, provided the original work is properly cited, the use is non-commercial and no modifications or adaptations are made.

© 2023 The Authors. *Journal of Raman Spectroscopy* published by John Wiley & Sons Ltd.

SSLs composed of a mixture of nonpolar lipids of epidermal and sebaceous origin^[9]: Triglycerides (TG) (20–60%), wax esters (23–29%), squalene (10–14%), free fatty acids (FFA) (5–40%), small amounts of cholesterol and cholesterol esters (1–5%), and diglycerides (DG) (1–2%).^[8,10–12]

The penetration of UV light through the skin leads to the formation of free radicals, which immediately interact with living cells. The generated free radicals can cause oxidation of epidermal proteins, lipids, and epidermal DNA.^[13–19]

While the protective properties of the skin against solar radiation are mainly based on melanin and *stratum corneum* components, SSLs are also involved in this barrier.^[20–26] They represent the first target of UV and other environmental radiations during natural or therapeutic exposure.^[27]

UV absorption by SSLs was evidenced by spectrophotometry with maximal absorption at 215 nm and an estimation of a 10% reduction of the transmission at 300 nm.^[28]

Besides representing a first line of defense by direct UV absorption, SSLs constitute a suitable target and scavenger for all reactive oxygen species (ROS) generated in the skin by different molecular mechanisms, during irradiation.^[29]

In addition to SSLs, the hydrolipidic film also contains antioxidants that protect the skin from the negative effects of oxidative stress. Among these, vitamin E has been identified as the main antioxidant in human skin, which can capture ROS.^[30,31]

This paper is the third part of a study that aimed to evaluate the impact of solar radiation on SSLs using vibrational spectroscopy. In the first and second parts, cumulative doses were applied on FFA and TG with different number of double bonds in the alkyl chains. In this paper, the effect of cumulative doses of solar radiation were studied on squalene (SQ), cholesterol (Chol), and a wax ester (WE: Palmitoleyl Palmitate). The behavior of vitamin E (VitE) was also monitored.

Finally, natural human extracts of SSLs were irradiated and analyzed by Raman spectroscopy to follow the step wise evolution of vibrational descriptors. High temperature gas chromatography coupled to mass spectrometry (HT-GC/MS) was also used to identify the first targets of solar radiation among the lipid classes of the SSLs.

2 | MATERIALS AND METHODS

2.1 | Chemicals

Squalene, cholesterol, and vitamin E (α -tocopherol) were purchased from Sigma Aldrich (St Louis, MO, United

states). Palmitoleyl Palmitate (16:1(9Z)/16:0) was purchased from Larodan (Solna, Sweden).

Human SSLs extracts were provided from the Center of Research Pierre Fabre Dermo Cosmetics (PFDC, Toulouse, France). Chloroform was purchased from Carlo Erba (Chaussée du Vexin, Val-de-Reuil, France).

For Raman measurements, lipids were dissolved in chloroform to obtain solutions of 2 mg/mL concentration; 20 μ L of each solution was deposited on CaF₂ slides. The lipid films were then dried to remove residual solvent traces.

For HT-GC/MS analyses 250 μ L of SSLs solution was prepared in chloroform. SSLs were derivatized in prior by trimethylsilylation. This reagent consisted of BSTFA/pyridine, 50:50 (v/v). SSLs were trimethylsilylated at room temperature for 30 min with 200 μ L of reagent. The excess reagent was then removed under nitrogen flow, and the dried residue was dissolved in 250 μ L of chloroform.

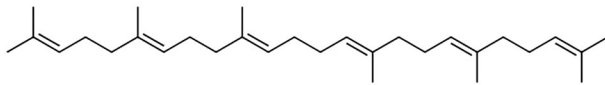
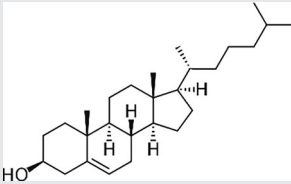
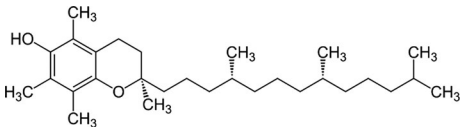
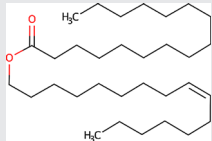
2.2 | Samples irradiation

Samples were irradiated at different times using a solar simulator 16S-300 (Solar Light, Glenside, Pennsylvania, USA), which produces a spectrum close to the solar spectrum at the sea level. The power used for the irradiation was 0.45 W/cm². This power was measured using a pyranometer (Glenside, USA). Table 1 shows the different energies used during the irradiation process.

2.3 | Raman spectroscopy

Raman spectral acquisitions were performed with an HR Labram microspectrometer (Horiba scientific, Palaiseau France). The excitation source is a 633-nm single-mode diode laser (TOPTICA PHOTONICS, Germany) with 35-mW laser power on the sample. The microspectrometer is equipped with an Olympus microscope, and measurements were recorded using a $\times 100$ MPlan objective (Olympus, Japan). Light scattered by the sample is collected through the same objective. A Peltier cooled (-65°C) multichannel coupled charge device (CCD) detector (1024 \times 256 pixels) detects the Raman Stokes signal dispersed with a 400- μ m slit width and a 600 grooves per millimeter holographic grating enabling a spectral resolution of 2 cm⁻¹. A calibration procedure was applied daily prior to data collection as recommended by Horiba Scientific. The zero-order position and the laser line were daily checked. Raman relative shift was checked on silica wafer band at 521 cm⁻¹. For the study, the selected spectral range was 400–3800 cm⁻¹.

TABLE 1 The lipids used in this study.

Lipids	Formula	Structure
Squalene	$C_{30}H_{50}$	
Cholesterol	$C_{27}H_{46}O$	
Vitamin E	$C_{29}H_{50}O_2$	
Palmitoleyl Palmitate	$C_{36}H_{62}O_2$	

The acquisition of each spectrum required 3 min. Spectral acquisition was performed using Labspec6 software (Horiba Jobin Yvon SAS, Lille, France).

2.4 | FTIR measurement

Spectral data were recorded using a Spotlight 400 infrared Spectrum (Perkin Elmer Life Sciences, Great Britain) equipped with a liquid nitrogen cooled 16-pixel mercury cadmium telluride (MCT) line detector. Before each acquisition, a background was recorded on a clean part of the CaF_2 slide. All spectra were recorded in the mid infrared region (4000 to 750 cm^{-1}) at 30 scans/spectrum with a spectral resolution of 2 cm^{-1} .

Nine different spectra were recorded for each slide. Data were preprocessed using Spectrum Image software.

2.5 | High temperature gas chromatography-mass spectrometry (HTGC-MS)

A Thermo Scientific (Austin, TX) gas chromatography unit (Trace GC Ultra) equipped with an on-column injector was coupled to a quadrupole DSQII mass spectrometer via a high-temperature interface. The separation was achieved using a $30\text{ m} \times 0.32\text{ mm}$ ZB-5HT capillary

column (Phenomenex, Torrance, CA) coated with $0.1\text{ }\mu\text{m}$ of 5% diphenyl/95% dimethylpolysiloxane, connected to a 5-m 0.32-mm HT-deactivated tubing guard column.

Helium was used as a carrier gas at a constant flow of 2 mL/min . The injector and transfer line temperatures were set to 80°C and 350°C , respectively. The oven temperature was programmed from 60°C to 240°C at 5°C/min ; 240°C to 320°C at 2.5°C/min ; and 320°C to 350°C at 1°C/min . The operating conditions for electronic impact mass spectrometry (EI-MS) were source temperature at 250°C , ionizing energy at 70 eV , and scan range from m/z 45 to 1000 with a period of 1 s. EI mass spectra were recorded in the total ion current (TIC) monitoring mode.

2.6 | Data analysis

IR and Raman data were analyzed with a software developed in-house, which operates in the Matlab environment (The Mathworks, Inc., Natick, MA, USA). The background, due to the fluorescence, was corrected using a polynomial function with a polynomial order of 4.^[32] All spectra were smoothed using Savitzky-Golay filter on 9 points with a polynomial order of 4 and normalized to the AUC of the CH stretching band. Automatic determination of the peak positions was performed using second derivatives.

3 | RESULTS AND DISCUSSION

3.1 | Squalene

Squalene (SQ) is suggested to be the initial target of skin lipid oxidation.^[33] It is considered as the major photoprotective component of SSLs and works as sacrificing antioxidants.^[34]

SQ ($C_{30}H_{50}$) is a lipid that is highly sensitive to oxidation. This property is obviously linked to the presence of six carbon double bonds ($C=C$), making it the most unsaturated molecule in the SSLs.^[35]

The first step of the oxidation process of SQ involves hydrogen abstraction from the CH_2 groups rather than the CH_3 groups, which is expected since the C-H positions adjacent to a double bond are known to be especially vulnerable to oxidation.^[36,37]

In an SSL mixture, hydrogen abstraction from SQ can be produced either by direct solar radiation, or by free radicals in particular peroxy radicals produced during the oxidation of poly unsaturated fatty acids (PUFA)

given that squalene is an important antioxidant that inhibits lipid peroxidation by scavenging peroxy and oxygen singlet radicals.^[38–41]

Thus, to confirm that direct solar radiation can be initiators of the first step of the oxidation process of SQ, this latter was irradiated and then analyzed using vibrational spectroscopy.

As known, the bands at around 2850 and 2920 cm^{-1} are associated with the symmetric and asymmetric CH_2 stretching, respectively, in infrared spectra, while in Raman, these bands occur at around 2850 and 2880 cm^{-1} for CH_2 symmetric and asymmetric stretching, respectively.^[42,43] CH_3 symmetric and asymmetric stretching bands occur near 2870 and 2950 and cm^{-1} , respectively, in infrared spectra and at around 2934 and 2962 cm^{-1} in Raman spectra.

The loss in CH_2 numbers was observed by the decrease of the $\nu(CH_2)/\nu(CH_3)$ ratio in both infrared and Raman spectra (Figures 1A and 2A). For higher doses, this decrease may be also related to the decomposition of alkyl chains into shorter compounds.

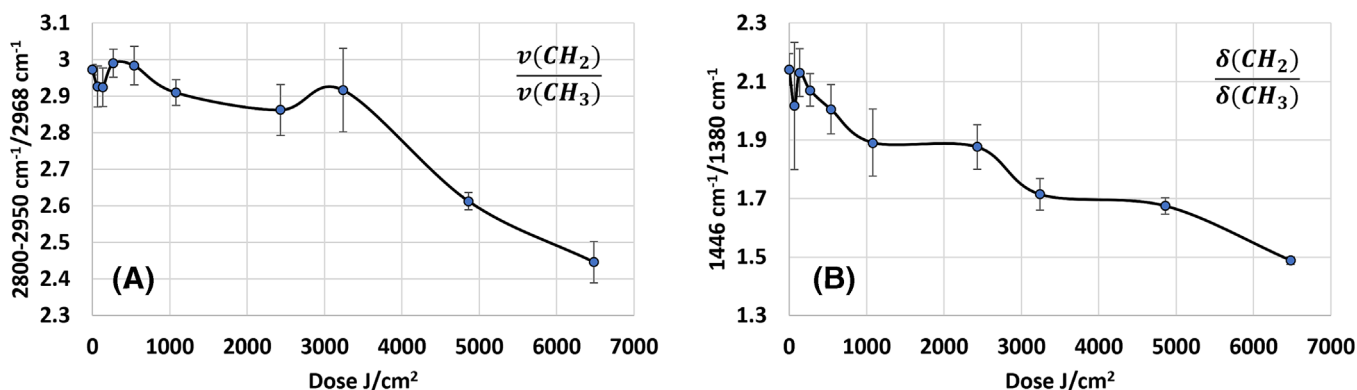


FIGURE 1 Infrared descriptors of squalene oxidation [(A) $\nu(CH_2)/\nu(CH_3)$, (B) $\delta(CH_2)/\delta(CH_3)$]. [Colour figure can be viewed at wileyonlinelibrary.com]

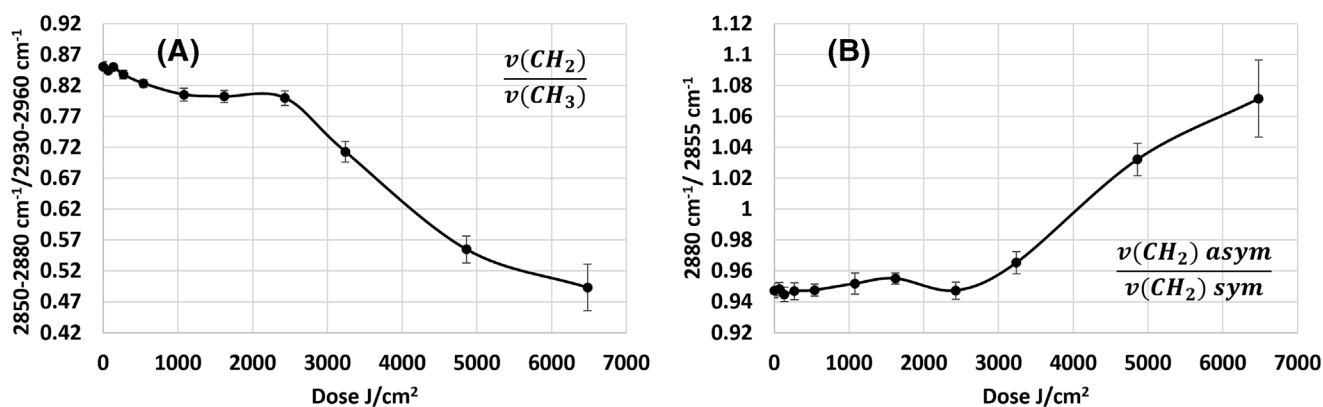


FIGURE 2 Raman descriptors of squalene oxidation [(A) $\nu(CH_2)/\nu(CH_3)$, (B) $\nu(CH_2) \text{ asym}/\nu(CH_2) \text{ sym}$].

This decrease in CH_2 numbers was confirmed by following the CH_2 scissoring to CH_3 bending ratio ($1446\text{ cm}^{-1}/1380\text{ cm}^{-1}$) in infrared spectra (Figure 1B).^[44]

After hydrogen abstraction, the oxygen attack would produce hydroperoxides, the primary oxidation products. The formation of hydroperoxides after a dose of 2430 J/cm^2 was confirmed by the appearance of a new absorption band assigned to OH stretching in the $3200\text{--}3600\text{ cm}^{-1}$ region (Figure 3C) and a shoulder at around 1070 cm^{-1} , assigned to C-O stretching of alkyl peroxides, in infrared spectra (Figure 3A).^[45]

In addition, an increase in the intensities at 850 cm^{-1} was observed in Raman spectra. This could be related to the O-O stretching (Figure 4A).^[45]

Hydroperoxides and peroxy radicals are unstable; a cyclization mechanism takes promptly place and lead to their decomposition and the production of the secondary oxidation products. The cyclization induces a reduction in the number of double bonds.

The reduction in the degree of SQ unsaturation was observed by the decrease in the AUC at 1667 cm^{-1} ($\nu(\text{C}=\text{C})$ stretching) in Raman spectra (Figure 4B). This was also confirmed by the decrease of the band assigned

to the vinyl CH stretch that arises at about 3010 and 3050 cm^{-1} , respectively, in Raman and infrared spectroscopy.

The final steps of the oxidation mechanisms lead to the formation of aldehydes including formaldehyde and malonaldehyde,^[46,47] ketones, alcohols, and other secondary products.^[33,44] This was observed by the appearance of an overlap of many bands in the carbonyl region ($1600\text{--}1800\text{ cm}^{-1}$) in infrared spectra, indicating that many functional groups containing carbonyl groups have been formed (Figure 3B). This was confirmed in Raman spectra by the appearance of a band at around 675 cm^{-1} after an irradiation dose of 3240 J/cm^2 . This band can be assigned to C-CO-C stretching vibration (aliphatic ketones) and C-C-CO in plane bending vibration (aliphatic aldehydes) (Figure 4A).^[45]

In addition, the appearance of a band in infrared spectra at around 1250 cm^{-1} (OH bending) at the same dose (3240 J/cm^2) (Figure 3A) indicated the formation of alcohols as secondary oxidation products.

In addition to the structural evolution, organizational and conformational changes were observed. An increase in the ($\nu(\text{CH}_2)$ asym/ $\nu(\text{CH}_2)$ sym) ratio in Raman spectra after oxidation was observed indicating a high

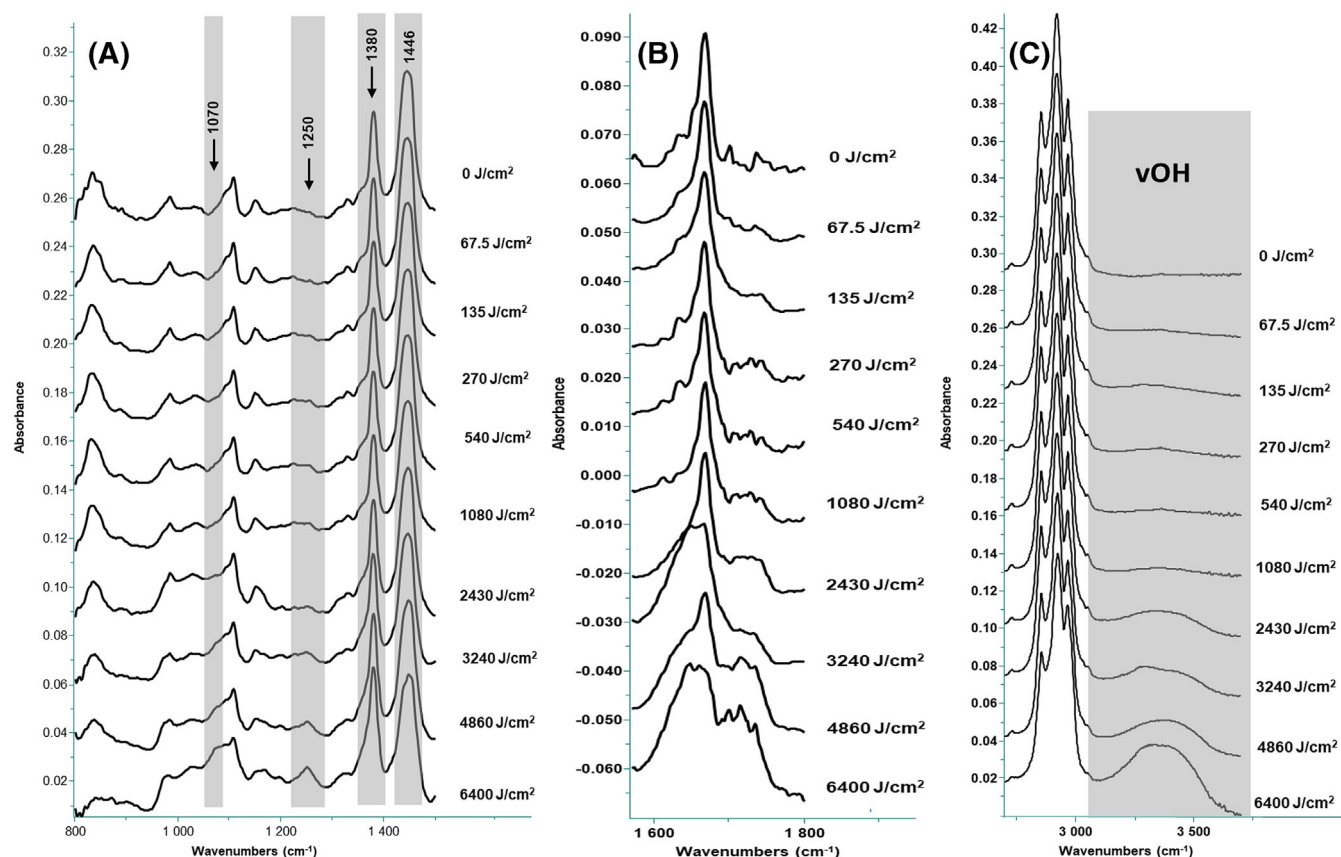


FIGURE 3 (A–C) Infrared spectra of squalene at different doses. [Colour figure can be viewed at wileyonlinelibrary.com]

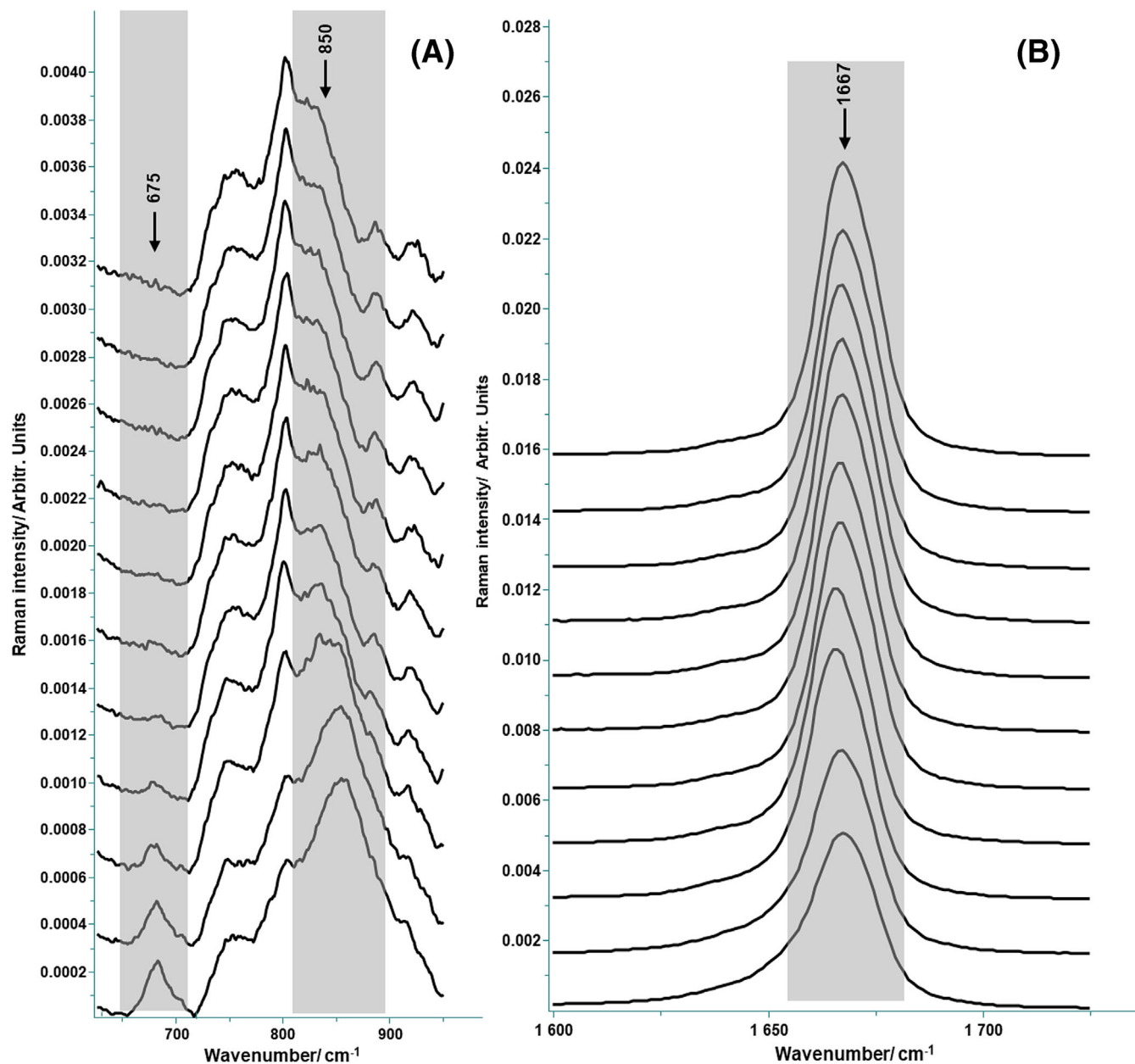


FIGURE 4 Raman spectra of squalene at different doses. [Colour figure can be viewed at [wileyonlinelibrary.com](https://onlinelibrary.wiley.com/doi/10.1002/jrs.6504)]

conformational order, that can be explained by the loss of double bonds (Figure 2B).

It is worthy to note that the oxidation descriptors observed in Figures 1 and 2 showed a significant evolution only after an applied dose of 2500 J/cm^2 , which means that the oxidation process started only from this dose. In the first part of this work,^[48] we have shown that the oxidation markers of PUFA evolved after application much lower solar doses, which confirmed that they oxidize faster than squalene. This can be explained by the fact that, unlike PUFA, such as sebaleic acid and linolenic acid, squalene does not have bis-allyl hydrogen,

making it relatively stable.^[14] More importantly, this indicated that in an SSL mixture, PUFA oxidation products promptly produced can be scavenged by the squalene.^[38–41]

3.2 | Cholesterol

Cholesterol has a characteristic arrangement of four interconnected cycloalkane rings, one of which is attached to the hydroxyl group in the third position, while the other end of this molecule is a side chain with eight carbon atoms (Table 1).^[49]

Infrared and Raman spectra of free cholesterol show different features (Figure 5). The bands between 2800 and 3000 cm^{-1} are associated with the asymmetric and symmetric stretching vibrations of CH_2 and CH_3 groups in Raman and infrared spectroscopy.^[49,50] The intense and broad band at 3400 cm^{-1} in infrared spectra is attributed to OH stretching.^[50] Cholesterol has one double band ($\text{C}=\text{C}$) in the second ring. It is prominently shown at 1670 cm^{-1} in Raman spectrum. The band at 1440 cm^{-1} in Raman spectra is attributed to the CH_2 scissoring, and the bands at 1378 and 1464 cm^{-1} are assigned to the CH_2 and CH_3 bending vibration of cholesterol molecule. In the lower wavenumber range of Raman spectra, several almost equally intense bands are seen at 1087, 1124, and 1176 cm^{-1} , associated with the C-C stretching modes. In addition, the bands that appear in the 800–1000 cm^{-1} region, are also associated to the C-C vibrational modes.^[49] The range between 400 and 800 cm^{-1} in Raman spectra is characteristic for cholesterol. Thus, the band at 701 cm^{-1} is associated with the in-plane bending of the ring, whereas the bands at

424 and 548 cm^{-1} are assigned to the bending vibrations of the C-H groups in the chain and rings.^[49]

In addition, the sharp peak at 1055 cm^{-1} in infrared spectra can be assigned to the ring deformation of cholesterol.^[50]

The chemical oxidation of cholesterol is frequently initiated by reactions involving ROS in particular free radicals such as lipid peroxyl radicals generated from the oxidation of PUFA that may react with cholesterol to form cholesterol peroxyl radicals, which are precursors of several cholesterol oxidation products.^[51]

The interaction of cholesterol with peroxyl radicals leads to the abstraction of the hydrogen from the C-7 (reactive site in the first oxidation step of cholesterol) and the formation of cholesterol radical.^[52] The latter can react with oxygen to form a cholesterol peroxyl radical. This radical can abstract a hydrogen from other lipid molecules leading to the formation of a relatively stable cholesterol hydroperoxide.^[53]

PUFA oxidize faster than cholesterol under direct solar radiation, because the abstraction of a hydrogen

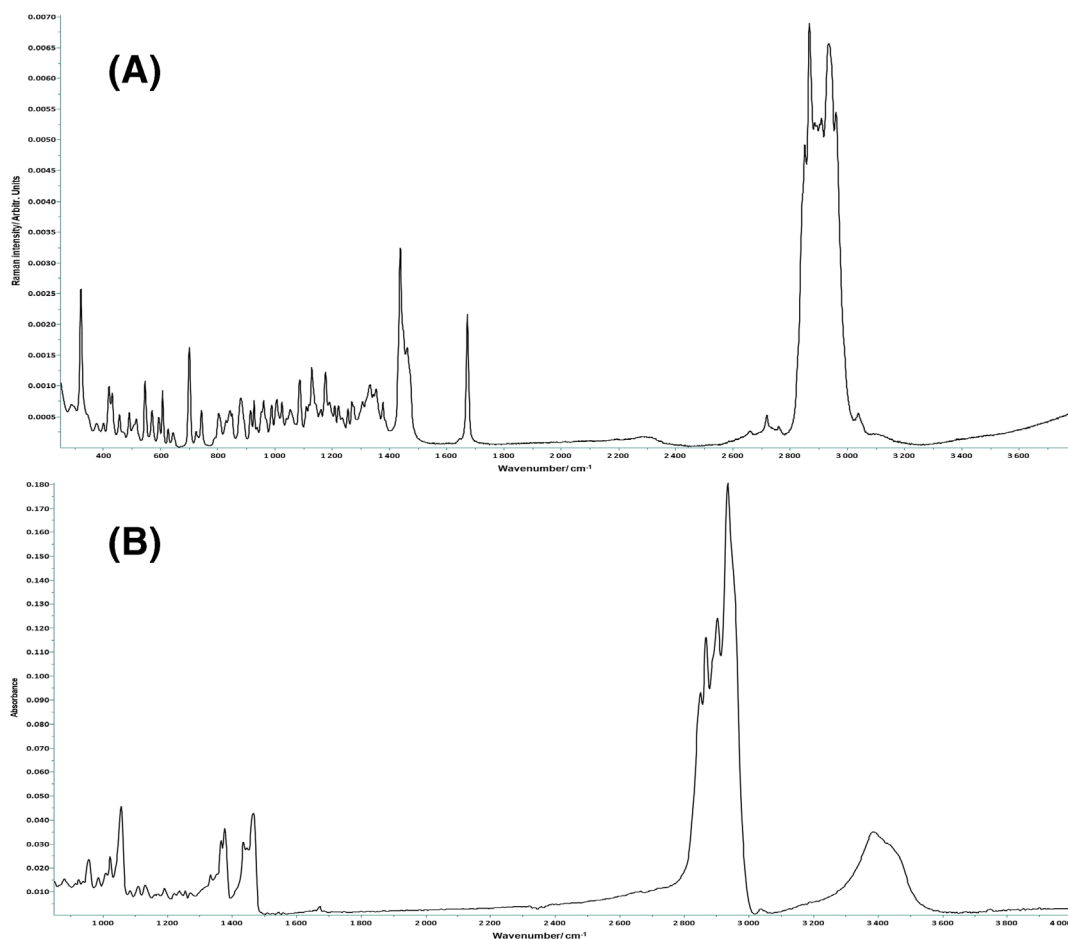


FIGURE 5 Raman (A) and infrared (B) spectra of cholesterol before oxidation. [Colour figure can be viewed at wileyonlinelibrary.com]

from the methylene group in PUFA (bis-allylic) would be thermodynamically more favorable than hydrogen abstraction from the C7 methylene group of cholesterol.^[54]

Thus, to study the direct impact of solar radiation, and to confirm that the hydrogen abstraction is mostly

due to the interaction with free radicals, cholesterol was directly irradiated and analyzed using vibrational spectroscopy.

No modifications were observed in Raman and infrared spectra after an irradiation dose of 6400 J/cm². This can confirm that the oxidation of cholesterol is

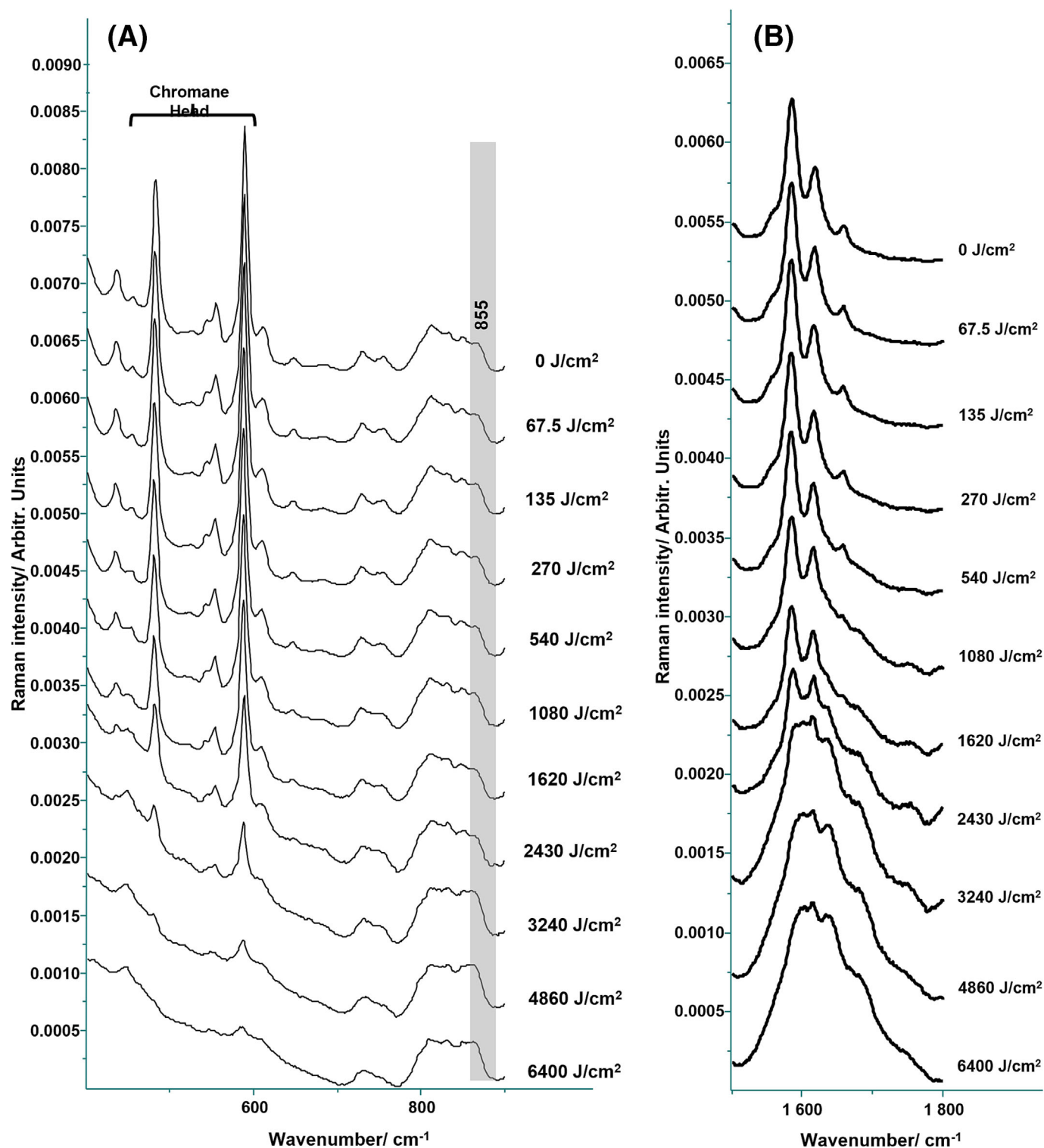


FIGURE 6 (A–B) Raman spectra of vitamin E at different doses. [Colour figure can be viewed at wileyonlinelibrary.com]

initiated (hydrogen abstraction) by free radicals including peroxy radicals generated from PUFA during their oxidation and one can conclude that cholesterol may act as an antioxidant like vitamin E by capturing free radicals and quenches lipid peroxidation chain reaction.

3.3 | Wax esters

Wax esters are formed by combining one fatty acid with one fatty alcohol. Waxes could be saturated and unsaturated in which the acid moiety and/or the alcohol moiety could be unsaturated.^[20] Only chains with two or more double bonds are prone to oxidation. Saturated and monosaturated ones are less vulnerable to lipid peroxidation than their unsaturated counterparts.^[55]

Only random nonsignificant variations in the $2885/2850\text{ cm}^{-1}$ ($\nu(\text{CH}_2)$ asym/ $\nu(\text{CH}_2)$ sym), the $1655\text{--}1675\text{ cm}^{-1}/2840\text{--}2890\text{ cm}^{-1}$ ($\nu(\text{C}=\text{C})/\nu(\text{CH})$), the

$972\text{ cm}^{-1}/2840\text{--}2890\text{ cm}^{-1}$ ($\delta(\text{=CH})/\nu(\text{CH})$), and the $1266\text{ cm}^{-1}/2840\text{--}2890\text{ cm}^{-1}$ ($\delta(\text{=CH})/\nu(\text{CH})$) ratios were observed in Raman spectra (data not shown).

3.4 | Vitamin E

Alpha tocopherol is the major biologically active vitamin E homolog. It has a chromane ring and a saturated hydrocarbon chain. There are eight methyl groups in alpha tocopherol, which four are attached to the chromane head and the other four are attached to the hydrocarbon chain. This molecule contains 11 methylene groups.^[56]

Raman and infrared spectra of vitamin E were collected and presented characteristic features. In the $1500\text{--}1800\text{ cm}^{-1}$ region, the observed bands at around 1585 and 1617 cm^{-1} in Raman spectra are assigned to the C-C stretching vibrations of the ring part of chromane

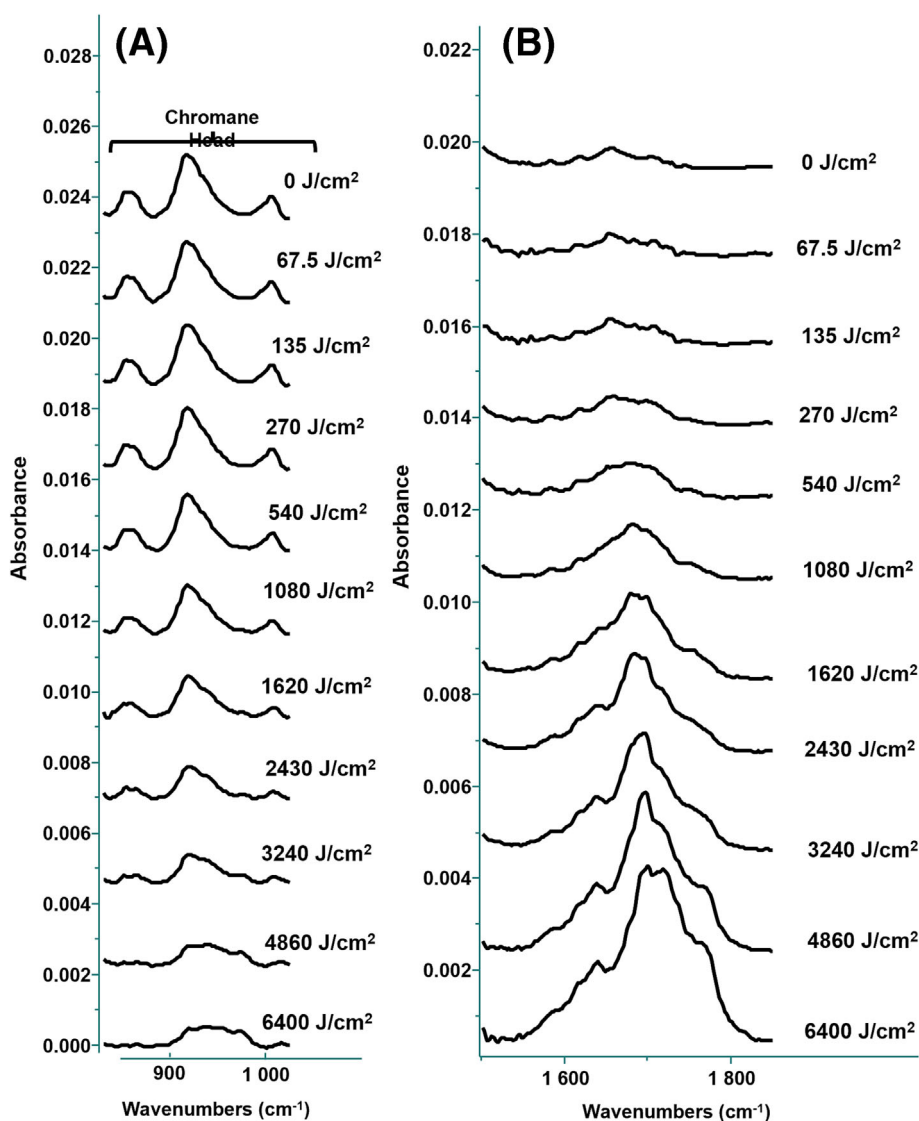


FIGURE 7 (A–B) Infrared spectra of vitamin E at different doses. [Colour figure can be viewed at [wileyonlinelibrary.com](https://onlinelibrary.wiley.com)]

head.^[56,57] The 950–1500 cm⁻¹ region is generally dominated by the wagging, scissoring, twisting, and rocking vibrations of CH₂ and CH₃ groups. In addition, bands assignable to the stretching vibrations of C-O and C-C also appear in this region. Finally, the region below 950 cm⁻¹ has main contribution from torsion, rocking, and bending modes and especially the bands assignable to the chromane head vibration.^[56,57]

Oxidation mechanisms of vitamin E with peroxy radicals, superoxide radical, and singlet oxygen have been extensively studied.^[58,59] It is generally regarded as the most important lipid-soluble antioxidant in human tissues such as skin. It prevents the propagation of lipid peroxidation by scavenging highly reactive peroxy radicals that are quenched by the hydrogen of phenolic OH group of alpha-tocopherol leading to the formation of

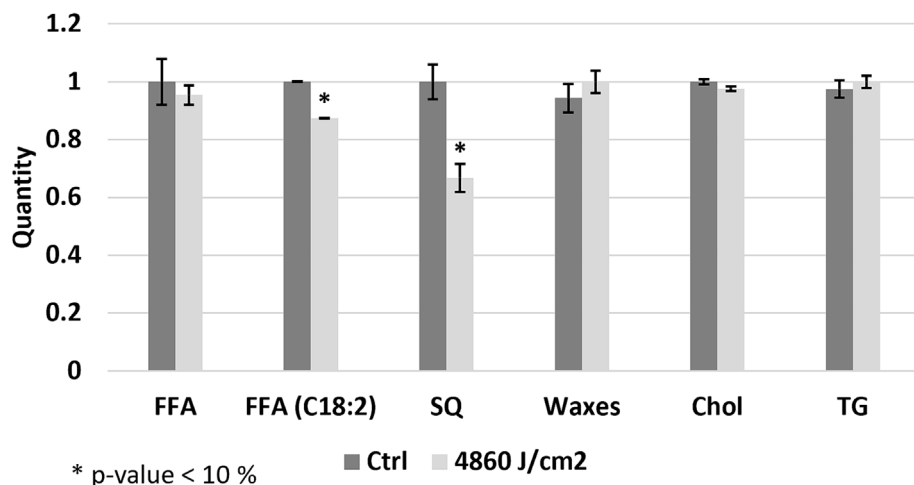


FIGURE 8 Histograms of the mean ($n = 3$) quantity of lipid classes of skin surface lipids (SSLs) before and after irradiation. Each lipid class quantity was normalized by the value before irradiation.

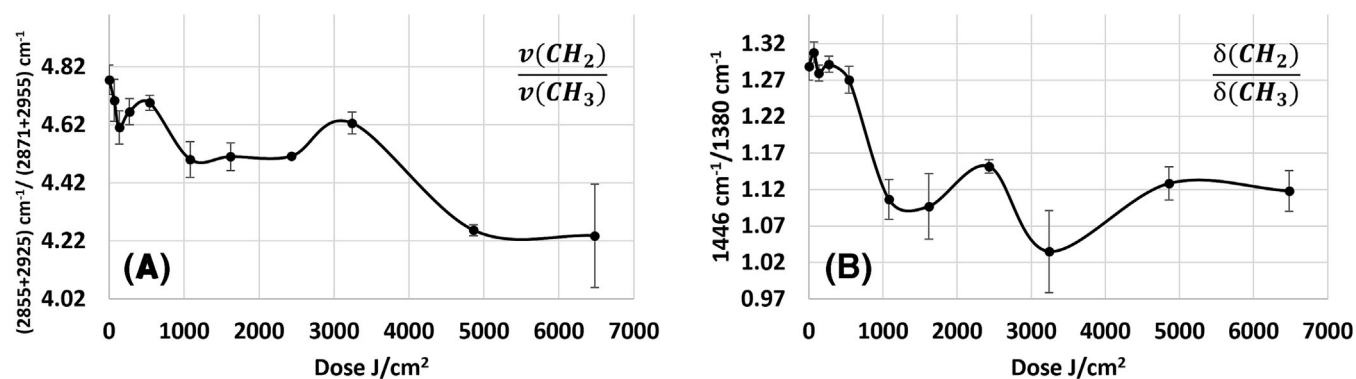


FIGURE 9 Infrared descriptors of skin surface lipids (SSLs) oxidation [(A) $v(CH_2)/v(CH_3)$, (B) $\delta(CH_2)/\delta(CH_3)$].

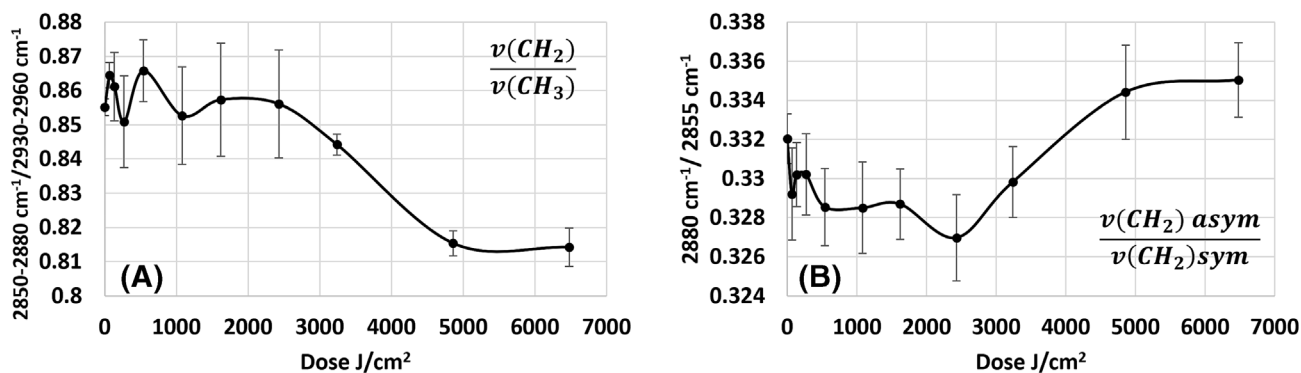


FIGURE 10 Raman descriptors of skin surface lipids (SSLs) oxidation [(A) $v(CH_2)/v(CH_3)$, (B) $v(CH_2)_{asym}/v(CH_2)_{sym}$].

alpha-tocopherol radical.^[60–63] The reaction of alpha-tocopherol radical with a second peroxy radical leads to the formation of many oxidation products such as quinones, epoxyquinones, ketones, and hydroperoxides that serve as markers of the antioxidant reactions of alpha-tocopherol.^[60,62–65]

Vitamin E oxidation can be also initiated by UV light with the abstraction of the hydrogen of the phenolic OH (homolytic cleavage of O–H bond) group, which leads to the formation of alpha-tocopherol radical and the oxidation mechanism begins.^[51]

Hence, to evaluate the direct impact of solar radiation, vitamin E was irradiated at different doses and was analyzed using infrared and Raman spectroscopy.

After solar irradiation (1620 J/cm²), a broadening in the 1500–1800 cm^{−1} region of Raman spectra was observed (Figure 6B). This broadening indicates the formation of oxidation products of alpha tocopherol that contain carbonyl function such as quinones, epoxyquinones, and ketones. The formation of these products was confirmed by the appearance of new bands in the 1500–1800 cm^{−1} region of infrared spectra (Figure 7B). In addition, an increase in the intensities at around 855 cm^{−1} in Raman spectra can be assigned to the O–O stretching (Figure 6A). This increase could be due to the formation of hydroperoxides after oxidation. Moreover, the disappearance of the bands below 950 cm^{−1} in Raman and infrared spectra may be due to chromane ring degradation after oxidation and the formation of oxidation products (Figures 6A and 7A).

3.5 | SSLs

Based on solar irradiations of different SSLs components individually, unsaturated FFA^[48] and unsaturated FA chains in triglycerides have shown an initiation of their oxidation process at lower doses than SQ. Meanwhile, it has been shown previously that when the human hydro-lipidic film is subjected to high-dose irradiations in vitro, SQ is significantly degraded compared with triglycerides, mono-di-unsaturated FFA, or cholesterol.^[29]

Thus, to confirm that SQ is the first target of solar radiation in SSLs and the more degraded, SSLs were irradiated for 3 h (4860 J/cm²) and then analyzed using HT-GC/MS (Figure 8).

The used HT-GC/MS method did not enable to detect vitamin E in the chromatogram. Thus, only SSLs were observed. As seen in Figure 8, no significant changes in the amount of the whole class of FFA, waxes, Chol, and TG were observed after irradiation. However, a marked

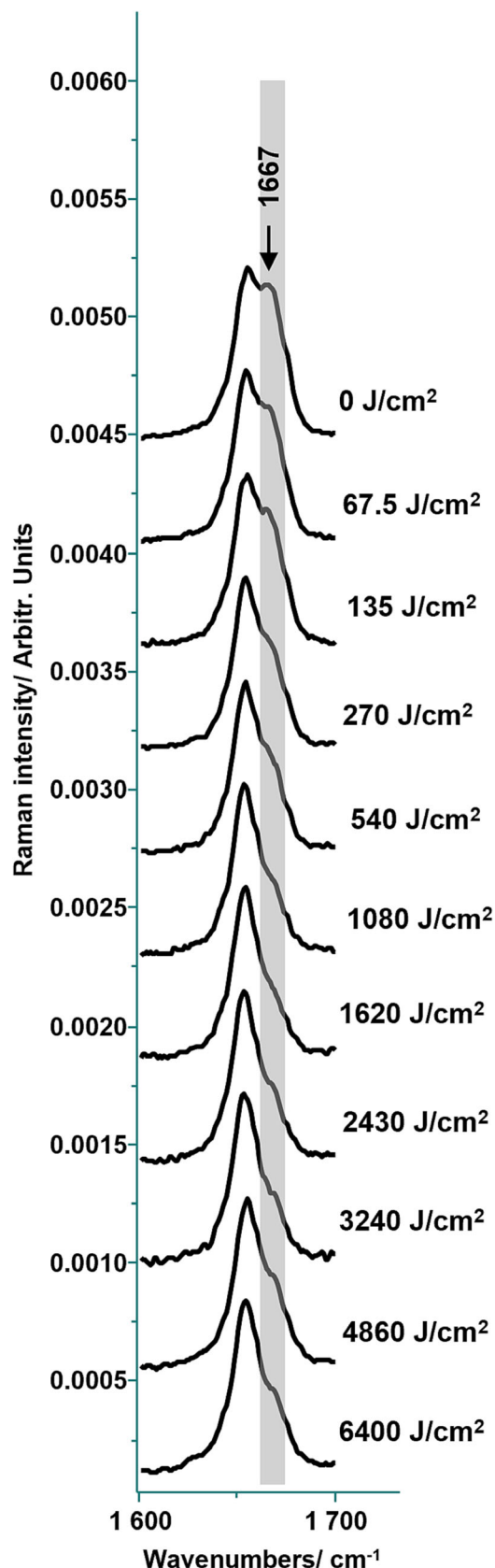


FIGURE 11 Raman spectra of vitamin E at different doses. [Colour figure can be viewed at wileyonlinelibrary.com]

TABLE 2 The different solar radiation doses applied to SSLs during irradiation in J/cm².

Time (min)	2.5	5	10	20	40	60	90	120	180	240
Total solar spectrum energy (J/cm ²)	67.5	135	270	540	1080	1620	2430	3240	4860	6480
UV-B energy (J/cm ²)	0.225	0.45	0.9	1.8	3.6	5.4	8.1	10.8	16.2	21.6
Minimal erythral dose	7.5 MED	15 MED	30 MED	60 MED	120 MED	180 MED	270 MED	360 MED	540 MED	720 MED

decrease of di-unsaturated FFA and a significant decrease of SQ were observed. The decrease in the amount of SQ was much more important than FFA (C18:2). This can be explained by the fact that SQ is the most abundant class in the SSLs,^[34] and due to its antioxidant role, PUFA oxidation products promptly produced can be scavenged by the SQ.

This confirms that in the SSLs, squalene is the first line defense against solar radiation and is the more oxidized component as compared to other lipidic classes. Furthermore, the behavior of lipid classes in SSLs against solar radiation may be different than if the lipids were irradiated individually.

In addition, SSLs were irradiated at different doses then analyzed using vibrational spectroscopy.

As previously mentioned, the first step of the oxidation involves hydrogen abstraction inducing a loss in CH₂ numbers that was observed by the decrease of the $\nu\text{CH}_2/\nu\text{CH}_3$ ratio in both, infrared, and Raman spectra of SSLs (Figures 9A and 10A).

This hydrogen abstraction was confirmed by the decrease of the 1446 cm⁻¹/1380 cm⁻¹ ratio (CH₂ scissoring)/(CH₃ bending) in infrared spectra (Figure 9B).

Infrared and Raman spectra obtained at different doses showed no detectable descriptors related to the production of hydroperoxides. However, a decrease in the intensity at 1667 cm⁻¹ was observed in the Raman spectra (Figure 11); this peak is assigned to the $\nu(\text{C}=\text{C})$ stretching of squalene in trans-conformation. The loss of unsaturation was confirmed by the decrease of the band assigned the =C-H stretching (vinyl CH stretch) that arises at about 3012 and 3050 cm⁻¹, respectively, in Raman and infrared spectroscopy.

Finally, an increase in the ($\nu(\text{CH}_2)$ asym/ $\nu(\text{CH}_2)$ sym) ratio in Raman spectra after oxidation was observed (Figure 10B). This evolution indicated a higher organizational order of SSLs film after irradiation.

4 | CONCLUSION

This paper is the third part of a study focused on the effect of solar radiation on SSLs. In the first part, PUFA showed direct oxidation after the application of low radiation doses. In the second part, the FA chains in triglycerides showed similar evolution with modification occurring more promptly compared to FFA.

In this part, when irradiated alone, SQ oxidation process was detectable only after 2430 J/cm² dose (Table 2). Similar observations were obtained for vitamin E (after 1620 J/cm²). No changes were observed on the cholesterol on the wax ester (Palmitoleyl Palmitate).

The HT-GC/MS analysis of extracted human SSLs did not enable to detect the vitamin E in the chromatogram. When extracted film was irradiated, the more marked modifications were observed on SQ in contrast to the irradiation of individual lipids.

The behavior of lipids under solar radiation was different either they were irradiated individually or in the mixture. In the SSLs mixture, a synergistic action took place. The abundance of squalene puts it in the first line of defense by absorbing a part of the energy of irradiation and by scavenging free radicals generated from the oxidation of PUFA. In addition to the antioxidant action of squalene and vitamin E within SSLs, SC contains various carotenoids with high antioxidant activity.^[66] It would be of great interest to extend investigations to better understand the behavior of lipids in the SSLs in presence of carotenoids.

ORCID

Ali Assi  <https://orcid.org/0000-0002-5019-0100>

REFERENCES

- [1] J. Bakar, R. A.-O. Michael-Jubeli, D. Libong, A. Baillet-Guffroy, A. Tfayli, *Anal. Bioanal. Chem.* **2022**, 414, 3675.
- [2] K. C. Madison, *J. Invest. Dermatol.* **2003**, 121, 231.
- [3] S. J. Jiang, J. Y. Chen, Z. F. Lu, J. Yao, D. F. Che, X. J. Zhou, *J. Dermatol. Sci.* **2006**, 44, 29.
- [4] F. F. Sahle, T. Gebre-Mariam, B. Dobner, J. Wohlrab, R. H. Neubert, *Skin Pharmacol. Physiol.* **2015**, 28, 42.
- [5] J. van Smeden, J. A. Bouwstra, *Curr. Probl. Dermatol.* **2016**, 49, 8.
- [6] V. Mlitz, J. Latreille, S. Gardinier, R. Jdid, Y. Drouault, P. Hufnagl, L. Eckhart, C. Guinot, E. Tschachler, *J. Eur. Acad. Dermatol. Venereol.* **2012**, 26, 983.
- [7] M. Gniadecka, H. C. Wulf, N. N. Mortensen, T. Poulsen, *Acta Derm. Venereol.* **1996**, 76, 429.
- [8] A. Rigal, R. Michael-Jubeli, A. Bigouret, A. Nkengne, D. Bertrand, A. Baillet-Guffroy, A. Tfayli, *Eur. J. Dermatol.* **2020**, 30, 103.
- [9] R. S. Greene, D. T. Downing, P. E. Pochi, J. S. Strauss, *J. Invest. Dermatol.* **1970**, 54, 240.
- [10] D. T. Downing, J. S. Strauss, *J. Invest. Dermatol.* **1974**, 62, 228.
- [11] M. E. Stewart, D. T. Downing, J. S. Cook, J. R. Hansen, J. S. Strauss, *Arch. Dermatol.* **1992**, 128, 1345.
- [12] A. Pappas, *Dermatoendocrinol* **2009**, 1, 72.
- [13] K. Biniek, K. Levi, R. H. Dauskardt, *Proc. Natl. Acad. Sci.* **2012**, 109, 17111.
- [14] E. Niki, *Free Radic. Res.* **2015**, 49, 827.
- [15] S. A. Thurstan, N. K. Gibbs, A. K. Langton, C. E. M. Griffiths, R. E. B. Watson, M. J. Sherratt, *Chem. Cent. J.* **2012**, 6, 34.
- [16] D. R. Bickers, M. Athar, *J. Invest. Dermatol.* **2006**, 126, 2565.
- [17] A. Nicolaou, M. Masoodi, K. Gledhill, A. K. Haylett, A. J. Thody, D. J. Tobin, L. E. Rhodes, *Photochem. Photobiol. Sci.* **2012**, 11, 371.
- [18] L. E. Rhodes, K. Gledhill, M. Masoodi, A. K. Haylett, M. Brownrigg, A. J. Thody, D. J. Tobin, A. Nicolaou, *FASEB J.* **2009**, 23, 3947.
- [19] C. Nishigori, Y. Hattori, S. Toyokuni, S. Toyokuni, *Antioxid. Redox Signal.* **2004**, 6, 561.
- [20] R. Michael-Jubeli, J. Bleton, A. Baillet-Guffroy, *J. Lipid Res.* **2011**, 52, 143.
- [21] J. W. Fluhr, M. Mao-Qiang, B. E. Brown, P. W. Wertz, D. Crumrine, J. P. Sundberg, K. R. Feingold, P. M. Elias, *J. Invest. Dermatol.* **2003**, 120(5), 728. <https://doi.org/10.1046/j.1523-1747.2003.12134.x>
- [22] A. Mavon, H. Zahouani, D. Redoules, P. Agache, Y. Gall, P. Humbert, *Colloids Surf. B* **1997**, 8, 147.
- [23] J. J. Thiele, S. U. Weber, L. Packer, *J. Invest. Dermatol.* **1999**, 113, 1006.
- [24] G. S. K. Pilgram, J. van der Meulen, G. S. Gooris, H. K. Koerten, J. A. Bouwstra, *BBA-Biomembranes* **2001**, 1511, 244.
- [25] M. Q. Man, S. J. Xin, S. P. Song, S. Y. Cho, X. J. Zhang, C. X. Tu, K. R. Feingold, P. M. Elias, *Skin Pharmacol. Physiol.* **2009**, 22, 190.
- [26] E. H. Choi, M. Q. Man, F. Fau-Wang, F. Wang, X. Fau-Zhang, X. Zhang, B. E. Fau-Brown, K. R. Brown Be Fau-Feingold, K. R. Feingold, P. M. Fau-Elias, P. M. Elias, *J. Invest. Dermatol.* **2005**, 125(2), 288. <https://doi.org/10.1111/j.0022-202X.2005.23799.x>
- [27] K. Hayakawa, I. Matsuo, *Tokai J. Exp. Clin. Med.* **1986**, 1(5), 317.
- [28] P. C. Beadle, J. L. Burton, *Brit J Dermatol* **1981**, 104, 549.
- [29] C. De Luca, G. Valacchi, *Mediators Inflamm.* **2010**, 2010, 321494.
- [30] L. Packer, G. Valacchi, *Skin Pharmacol. Physiol.* **2002**, 15, 282.
- [31] F. Nachbar, H. C. Korting, *J. Mol. Med. (Berl.)* **1995**, 73(1), 7. <https://doi.org/10.1007/BF00203614>
- [32] C. A. Lieber, A. Mahadevan-Jansen, *Appl. Spectrosc.* **2003**, 57(11), 363. <https://doi.org/10.1366/000370203322554518>
- [33] N. Shimizu, J. Ito, S. Kato, Y. Otoki, M. Goto, T. Eitsuka, T. Miyazawa, K. Nakagawa, *Sci. Rep.* **2018**, 8, 9116.
- [34] V. Kostyuk, A. Potapovich, A. Stancato, C. De Luca, D. Lulli, S. Pastore, L. Korkina, *PLoS ONE* **2012**, 7, e44472.
- [35] D. M. Pham, B. Boussouira, D. Moyal, Q. L. Nguyen, *Int. J. Cosmet. Sci.* **2015**, 37(4), 357. <https://doi.org/10.1111/ics.12208>
- [36] Y.-S. Chi, S. Kay Obendorf, *J. Surfactant Deterg.* **1998**, 1, 371.
- [37] Z. Y. Jiang, A. C. Woollard, S. P. Fau-Wolff, S. P. Wolff, *Lipids*, **1991**, 26(10), 853. <https://doi.org/10.1007/BF02536169>
- [38] Y. Kohno, Y. Egawa, S. Fau-Itoh, S. Itoh S. Fau-Nagaoka, S. Nagaoka, M. Fau-Takahashi, M. Takahashi, K. Fau-Mukai, K. Mukai, *Biochim. Biophys. Acta* **1995**, 1256(1), 52. [https://doi.org/10.1016/0005-2760\(95\)00005-w](https://doi.org/10.1016/0005-2760(95)00005-w)
- [39] F. Warleta, M. Campos, Y. Fau-Allouche, Y. Allouche, C. Fau-Sánchez-Quesada, C. Sánchez-Quesada, J. Fau-Ruiz-Mora, J. Ruiz-Mora, G. Fau-Beltrán, G. Beltrán, J. J. Fau-Gaforio, J. J. Gaforio, *Food Chem. Toxicol.* **2010**, 48(4), 1092. <https://doi.org/10.1016/j.fct.2010.01.031>
- [40] S.-K. Kim, F. Karadeniz, *Adv. Food Nutr. Res.* **2012**, 65, 223.
- [41] R. Amarowicz, *Eur. J. Lipid Sci. Technol.* **2009**, 111, 411.
- [42] E. Guillard, A. Tfayli, M. Manfait, A. Baillet-Guffroy, *Anal. Bioanal. Chem.* **2011**, 399, 1201.

- [43] A. Tfayli, E. Guillard, M. Manfait, A. Baillet-Guffroy, *Anal. Bioanal. Chem.* **2010**, 397, 1281.
- [44] E. Naziri, R. Consonni, M. Z. Tsimidou, *Eur. J. Lipid Sci. Technol.* **2014**, 116, 1400.
- [45] *J. Am. Chem. Soc.* **2002**, 124, 1830.
- [46] H. C. Yeo, T. Shibamoto, *J. Surfactants Deterg.* **1998**, 1(3), 371. <https://doi.org/10.1007/s11743-998-0038-y>
- [47] K. J. Dennis, T. Fau-Shibamoto, T. Shibamoto, *Lipids* **1991**, 26(10), 853. <https://doi.org/10.1007/BF02536169>
- [48] A. Assi, R. Michael-Jubeli, A. Baillet-Guffroy, A. Tfayli, *J. Raman Spectrosc.* **2022**, 54, 24.
- [49] K. Czamara, K. Majzner, M. Z. Pacia, K. Kochan, A. Kaczor, M. Baranska, *J. Raman Spectrosc.* **2015**, 46, 4.
- [50] U. Gupta, V. K. Singh, V. Kumar, Y. Khajuria, *Materials Focus* **2014**, 3, 211.
- [51] M. E. Medina, A. Galano, Á. Trigos, *J. Phys. Org. Chem* **2015**, 28, 504.
- [52] A. J. Brown, W. Jessup, *Mol. Aspects Med.* **2009**, 30, 111.
- [53] W. Kulig, L. Cwiklik, P. Jurkiewicz, T. Rog, I. Vattulainen, *Chem. Phys. Lipids* **2016**, 199, 144. <https://doi.org/10.1016/j.chemphyslip.2016.03.001>
- [54] L. Iuliano, *Chem. Phys. Lipids* **2011**, 164(6), 457. <https://doi.org/10.1016/j.chemphyslip.2011.06.006>
- [55] L. Rael, G. Thomas, M. Craun, C. Curtis, *J. Biochem. Mol. Biol.* **2004**, 37, 749.
- [56] G. Singh, R. Sachdeva, B. Rai, G. S. S. Saini, *J. Mol. Struct.* **2017**, 1144, 347.
- [57] T. Cai, H.-M. Gu, A. Liu, M. Xie, *Appl. Spectrosc.* **2012**, 66, 114.
- [58] *Lipid Oxidation Pathways* (Ed: A. Kamal-Eldin), 1st ed., AOCS Publishing, New York **2003**, 323. <https://doi.org/10.1201/9781003040316>
- [59] W. Yu, L. Yang, Z. L. Liu, *Chin. Chem. Lett.* **2022**, 9, 823.
- [60] K. A. Kramer, D. C. Liebler, *Chem. Res. Toxicol.* **1997**, 10(2), 219. <https://doi.org/10.1021/tx960163u>
- [61] S. Ekanayake-Mudiyanselage, A. Tavakkol, T. G. Fau-Polefka, T. G. Polefka, Z. Fau-Nabi, Z. Nabi, P. Fau-Elsner, P. Elsner, J. J. Fau-Thiele, J. J. Thiele, *Skin Pharmacol. Physiol.* **2005**, 18(1), 20. <https://doi.org/10.1159/000081682>
- [62] B. D. Pekiner, *Skin Pharmacol. Physiol.* **2005**, 18(1), 20. <https://doi.org/10.1159/000081682>
- [63] G. W. Grams, *Tetrahedron Lett.* **1971**, 12, 4823.
- [64] S. De Vaugelade, E. Nicol, S. Vujovic, S. Bourcier, S. Pirnay, S. Bouchonnet, *J. Chromatogr. A* **2017**, 1517, 126.
- [65] C. Tang, G. Tao, Y. Wang, Y. Liu, J. Li, *J. Agric. Food Chem.* **2020**, 68, 669.
- [66] M. A.-O. Darvin, J. A.-O. Lademann, J. von Hagen, S. B. Lohan, H. A.-O. Kolmar, M. C. Meinke, S. Jung, *Antioxidants* **2022**, 11(8), 1451. <https://doi.org/10.3390/antiox11081451>

How to cite this article: A. Assi, R. Michael-Jubeli, C. Jacques-Jamin, H. Duplan, A. Baillet-Guffroy, A. Tfayli, *J. Raman Spectrosc* **2023**, 1. <https://doi.org/10.1002/jrs.6504>